Extended Abstracts of the 2010 International Conference on Solid State Devices and Materials, Tokyo, 2010, pp894-895

Performance Evaluation of Graphene Nanoribbon Heterojunction Tunneling Field Effect Transistors with various Source/Drain Doping Concentration and Heterojunction structure

Haixia Da[1†], Kai-Tak Lam[1], Sai Kong Chin[2], Ganesh S. Samudra[1], Yee-Chia Yeo[1], and Gengchiau Liang[1†]
[1]Deparrtment of Electrical and Computer Engineering, National University of Singapore, Singapore
[2]Institute of High Performance Computing, Singapore
[†]Phone: +65-6516-2898 E-mail: eledah@nus.edu.sg, and elelg@nus.edu.sg

1. Introduction

The complementary metal-oxide semiconductor (CMOS) transistors based on silicon (Si) are reaching the fundamental limits. This drives considerable research on new channel materials and novel functional devices [1] to enable further increase in device density and reduction in supply voltage. The tunneling field-effect transistors (TFETs) are one of the potential candidates for low power consumption applications due to its ability to achieve sub-60 meV/decade subthreshold swing (SS). However, ON-state currents (I_{ON}) of Si based TFETs are much lower than the requirement [2] due to the relatively large bandgap and tunneling mass of carriers. Materials with smaller carrier tunneling mass and new TFET structures are required to enhance I_{ON}.

Recently, one dimensional armchair graphene nano-ribbons (AGNRs) have attracted great attention due to their unique benefits, such as higher carrier velocities and low carrier effective masses [3]. AGNRs can also be patterned to form heterojuction structures with non-uniform widths in resonant tunneling diodes (RTDs) and heterojunction TFETs (HJTFETs) devices [4-5]. Compared with the case of the homogeneous structure, GNR HJFETs are able to provide higher I_{ON} [5]. Hence, there is considerable interest to exploit and identify the optimum geometrical configuration in the HJTFET.

In this work, we present a computational study on how the *I-V* characteristics of HJTFET are influenced by doping concentrations in Source/Drain (S/D) region and geometrical parameters by performing the self-consistent nonequilibrium Green's function (NEGF) and quasi-2D Poisson solver [5-6].

2. Simulation Model

Fig. 1 shows the device structure and the top view of the GNR HJTFET, whose part of channel region is composed of GNR with a larger width to form the smaller bandgap. The width (W_{HJ}) and length (L_{HJ}) of this wider GNR shown in Fig. 1(b) is used as a parameter for optimization of HJGNR devices to achieve the better performance.

The device physics and performance is modeled by a mode-space quantum transport simulator based on the self-consistently non-equilibrium Green's function (NEGF) based on Dirac equation, and Poisson equation with surface potential approximation [5-6]. Transverse moment operator (k_y) in Dirac equation is treated as a particular mode-space parameter that corresponds to the same electronic band structures generated by the π–orbital tight-binding calculation of GNR within an energy range of interest.

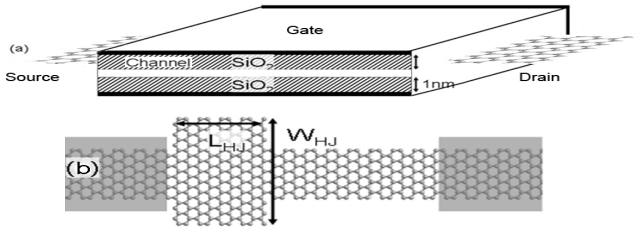

Fig. 1: (a) Schematic diagram of a double-gate heterojunction graphene nanoribbon tunneling field effect transistor. The gate insulator is silicon dioxide with a thickness (t_{ins}) of 1 nm in this work. (b) The top view of the GNR HJTFET. The source and drain are doped with holes and electrons respectively and different ribbon width in the channel are used. The channel length of the device is kept constant at 16 nm.

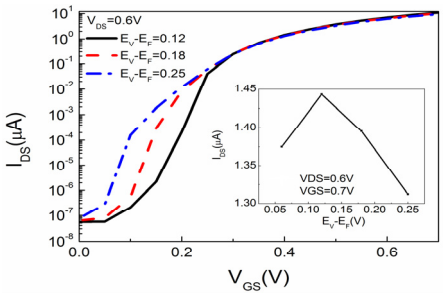

Fig. 2: The *I-V* characteristics of GNR HJTFET with different doping concentrations of (a) 3.83×10^{8} m^{-1} (black, solid), (b) 4.98×10^{8} m^{-1} (red, dash) and (c) 7.10×10^{8} m^{-1} (blue, dash-dot).

3. Results and Discussion

Firstly, we investigate the effects of different doping level in the S/D on device performance. We consider the device structure with intrinsic doped channel and the source (drain) as the heavily p-type (n-type) to form a *p-i-n* structure. Fig. 2 presents the I_{DS}-V_{GS} characteristics at different doping concentration $N_s = N_d = 3.83$, 4.98 and 7.10×10^{8} m^{-1} (which is defined by $E_V - E_F$ =0.12, 0.18 and 0.25eV) by solid, dashed, and dash-dotted curves, respectively. The value of SS depends strongly on doping concentration. It can be attributed to tunneling contributed by thermal electrons. With increasing doping concentration is high, i.e. the larger $E_V - E_F$ window, the thermal electrons can play an important role to determine the subthreshold current like the MOSFETs, resulting in increasing SS.

Furthermore, we observe another interesting phenomenon which is contrary to the characteristics of homogenous TFETs whose lowest OFF-state current (I_{OFF}) and I_{ON} monotonically decreases as doping concentration decreases. From Fig. 2, we find in the cases of HJ TFETs, I_{OFF} roughly remains constant with the different doping concentrations, and I_{ON} slightly increases (inset) as doping levels decreases. The reason of the latter can be attributed to

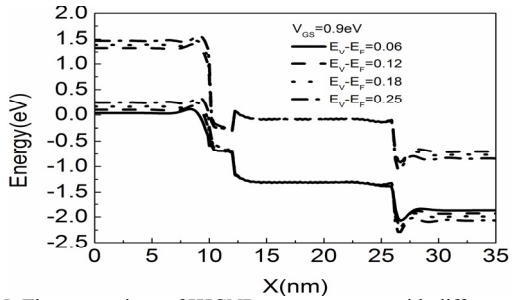

Fig. 5: The comparison of HJGNR energy spectra with different doping level of 0.06, 0.12, 0.18 and 0.25. V_{DS} is set as 0.6V.

the competition between the tunneling width and the available injection carriers around the Fermi level at the source side. Based on the quantum transport's point of view, the current is contributed by the available states and the tunneling rates. Although as doping concentration decreases, the tunneling width increases, this effect is diminished by HJ structure. Furthermore, due to the unique feature of 1D material, the density of state always peaks at the subband edge. Coupled with the effect of the Fermi distribution, more electrons are available to transport in the low doping cases. Therefore, I_{ON} slightly increases.

Next, we explore the geometry effects of the HJ structure with the different width (W_{HJ}) and length (L_{HJ}) on device performance. First, L_{HJ} is fixed to 2.0 nm and W_{HJ} is varied from 2.2 to 3.3 nm. As shown in Fig. 4, I_{ON} increases by 37% with the increase of W_{HJ} from 2.2 to 3.3 nm, while the I_{OFF} remains relatively constant at the order of 10^{-8} mA/μm. The changes of I_{ON} and I_{OFF} can be understood by the band-to-band tunneling mechanism (BTBT). As V_{GS} increases, the E_C and E_V at the channel-drain interface is being pulled apart and the BTBT at the drain side decreases, and at V_{GS} = 0.3 V, the current is mainly due to the direct tunneling between the source and the drain, thus the constant I_{OFF} is due to the constant effective source to drain tunneling width. As V_{GS} increases further, the E_C of the channel is pulled below the E_V of the source and BTBT occurs at the source-channel interface. The increase in I_{ON} can be ascribed to this enhancement of the BTBT at the source-channel interface due to the decrease in E_G (ranging from 0.46 to 0.31 eV). Lastly, L_{HJ} is varied from 2 nm to 14 nm and W_{HJ} is fixed at 2.5 nm. As shown in Fig. 5, I_{ON} stays relatively constant in the range of few mA/μm, as the tunneling probability does not change much at the source-to-channel interface. On the other hand, I_{OFF} increases exponentially with L_{HJ} due to the decrease in the effective source-to-drain tunneling width as shown in Fig. 6. Clearly, the HJ region with smaller E_G should be as short as possible to minimize the degradation of I_{OFF} performance.

4. Conclusion

The influence of doping concentration and geometrical parameters on the current-voltage characteristics of HJ GNR TFETs has been theoretically investigated. Using Dirac NEGF approach, we have demonstrated that I_{ON} as well as *SS* can be enhanced by controlling the doping concentration. Furthermore, it has shown that the feasibility of improving the device performance by changing the geometrical parameters in the configuration. I_{ON} can be increased by increasing the width of the HJ region at the channel and the I_{OFF} can be decreased by shortening the length of the HJ region within the channel region. The results will facilitate the development of HJTFETs devices.

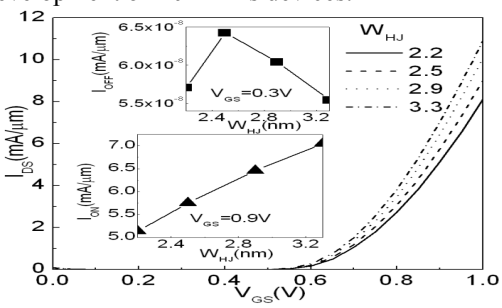

Fig. 4: The current characteristics of GNR HJ TFET at the different W_{HJ}. The upper and lower insets show the I_{OFF} and I_{ON} as a function of W_{HJ} respectively. There is a 37% increase in I_{ON} as W_{HJ} changes from 2.2 to 3.3 nm while the I_{OFF} decreases as W_{HJ} changes from 2.5 to 3.3 nm.

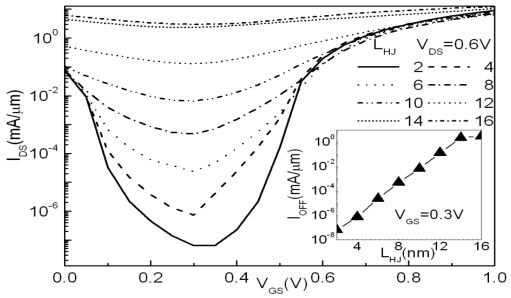

Fig. 5: The I_{DS}-V_{GS} characteristics of the HJ device as the length of the HJ region increases. The I_{ON} stays at the same order of magnitude while the I_{OFF} increases exponentially with the increase in L_{HJ}, as shown in the inset.

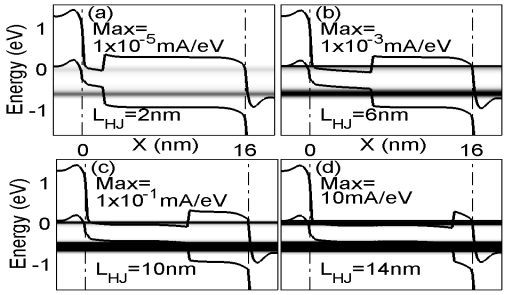

Fig. 6: The band diagram and current flux of the GNR HJ TFET at OFF-state with L_{HJ} equal to (a) 2, (b) 6, (c) 10, and (d) 14 nm to understand the increase in the I_{OFF}. The effective tunneling width for the S/D tunneling at OFF-state decreased with increasing L_{HJ}. This led to an increasing I_{OFF} as the S/D tunneling current increased. The plots have different maximum contrast (Max) which is shown in each plot.

Acknowledgments

This work was supported by the Agency for Science, Technology, and Research (A*STAR) under Grant no. 082-101-0023.

References

[1] "Process integration, devices, and structures," International Technology Roadmap for Semiconductors (ITRS) 2009. [Online]. Available: http://www.itrs.net/Links/2009ITRS/2009Chapters_2009Tables/2009_PIDS.pdf. [2] N. M. Niladri *et al.*, IEEE Transactions on Electron Devices, 56, 2193 (2009). [3] X. R.Wang *et al.*, Phys. Rev. Lett. 100, 206803 (2008). [4] H. Teong *et al.*, J. Appl. Phy. 105, 084317 (2009). [5] Kai-Tak Lam et al., IEEE Electron Device Lett., In Press (2010).[6] C. S. Koong et al. Jap. J. Appl. Phy. 49, 04DN07 (2010).